High-Performance Polyoxometalate-Based Cathode Materials for Rechargeable Lithium-Ion Batteries

Jia-Jia Chen, Mark D. Symes, Shao-Cong Fan, Ming-Sen Zheng, Haralampos N. Miras, Quan-Feng Dong, and Leroy Cronin**

Rechargeable lithium batteries show great promise for high-density energy storage for applications ranging from consumer electronics to electric vehicles and grid balancing.[1] Cathode materials in these batteries are typically oxides of transition metals, which undergo oxidation to higher valences when lithium is removed.[2] Current cathode materials for rechargeable Li-ion batteries are still mainly based on bulk transition metal oxides:[3] distorted rock-salt α-$NaFeO_2$ structures,[4] spinel structures,[5] and olivine structures.[6] However, either the low Li-ion mobility and/or the low electronic conductivity of these compounds hamper a high power density output, unless particle sizes are reduced to the nano-scale.[7] or carbon coating/doping strategies are employed.[8] In order to satisfy the increasing demand for high power density and energy density, new cathode materials capable of multielectron redox reactions and that enable more rapid Li-ion transportation (while still displaying stable cycling performance) are required.[9]

Recently, polyoxometalates[10] and metal–organic frameworks (MOFs)[11] have been shown to have potential as the cathode materials for rechargeable batteries. For example, $[Fe^{III}(OH)_{0.8}F_{0.2}(O_2CC_6H_4CO_2)]\cdot H_2O$ (MIL-53(Fe)$\cdot H_2O$) has been used as the cathode material for Li-based batteries, although the capacity was limited by the low number of electrons (not more than one electron per formula unit) involved in the reversible redox reaction.[12] Polyoxometalates are promising multifunctional materials which have numerous applications in catalysis, photoluminescence, as single molecule magnets, and as proton-conductive materials.[13] One of the most important features of POMs is the ability to configure or tailor their redox properties, which allows the development of new functional systems, such as metal–oxide–semiconductor (MOS) flash memory devices[14] and mediators for electrochemical water splitting.[15]

Polyoxometalates have already demonstrated some promise as the cathode in lithium batteries,[10] for example where the active cathode material was phosphomolybdate ($[PMo_{12}O_{40}]^{3-}$) and the anode was lithium metal.[10] In operando Mo K-edge XAFS measurements on these cathodes revealed that $[PMo_{12}O_{40}]^{3-}$ functioned as an "electron sponge," cycling reversibly by 24 electrons between $[PMo_{12}O_{40}]^{3-}$ and $[PMo_{12}O_{40}]^{27-}$ during charging/discharging.[16] However, the energy density and power density metrics of these cathode materials were limited by the slow rate of charge/discharge: capacities in excess of 200 mA h g^{-1} could be obtained after ten cycles, but only at a low current of 1 mA.

In view of this prior work, we hypothesized that vanadium-based polyoxometalates would make excellent cathode material candidates, exhibiting high capacities and rapid charging/discharging while also providing a larger operating voltage than the polyoxometalates previously explored for this purpose. Herein, we show that the polyoxovanadate $Li_7[V_{15}O_{36}(CO_3)]$ has multielectron redox properties suitable for producing cathode materials with a specific capacity of 250 mA h g^{-1}, and energy and power densities of 1.5 kW h L^{-1} and 55 kW L^{-1} respectively in Li-based batteries.

$Li_7[V_{15}O_{36}(CO_3)]$ was prepared according to an adapted literature procedure[17c] and its crystal structure is shown in **Figure 1**a. The spherical anion $\{V_{15}O_{36}\}$ of $Li_7[V_{15}O_{36}(CO_3)]$ has a "hollow sphere" structure with an encapsulated CO_3^{2-} group, which has the high crystallographic symmetry D_{3h}, formed by linkage of 15 tetragonal VO_5 pyramids. The 15 V atoms are arranged on the surface of a sphere at a distance of 343 ± 10 pm from the center of the cluster. $\{V_{15}O_{36}\}$ formally contains eight V^{IV} centers and seven V^{V} centers. Six VO_5 pyramids are each linked via three edges and two corners, six further are each linked via two edges and three corners, and three are each linked via two edges and four corners. All μ_3-O atoms concomitantly participate in two edge linkages and one corner-linkage; the μ_2-O atoms form a corner linkage. Such linkages lead to the formation of cubic cages with a cluster anion at each corner, which is further arranged along the three channels occupied by water and cations (see Figure S1 in the Supporting Information). These polyoxovanadate clusters also show good thermal stability when dried at 200 °C under vacuum overnight (Figure S2, Supporting Information). As shown in the TEM image of Figure 1b, the dehydrated polyoxovanadate clusters form ultrafine particles less than 5 nm in diameter, probably

Dr. J.-J. Chen, Dr. M. D. Symes, S.-C. Fan, Dr. M.-S. Zheng, Dr. H. N. Miras, Prof. Q.-F. Dong, Prof. L. Cronin
State Key Laboratory of Physical Chemistry of Solid Surfaces
Collaborative Innovation Centre of Chemistry for Energy Materials
Department of Chemistry
College of Chemistry and Chemical Engineering
Xiamen University
Xiamen, Fujian 361005, China
E-mail: qfdong@xmu.edu.cn; Lee.Cronin@glasgow.ac.uk
Dr. J.-J. Chen, Dr. M. D. Symes, Dr. H. N. Miras, Prof. L. Cronin
WestCHEM
School of Chemistry
the University of Glasgow
University Avenue
Glasgow G12 8QQ, UK

DOI: 10.1002/adma.201501088

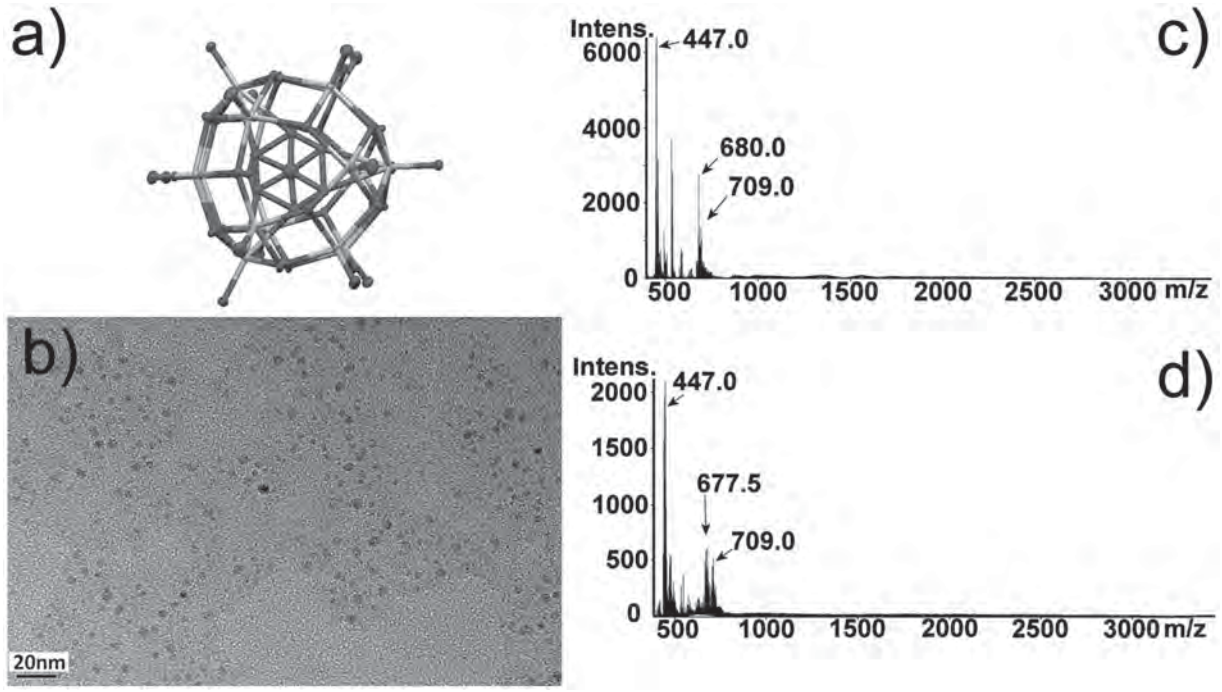

Figure 1. a) The crystal structure of $Li_7[V_{15}O_{36}(CO_3)]$, light gray: vanadium, dark gray: oxygen. b) TEM image of dehydrated nanoparticles of $Li_7[V_{15}O_{36}(CO_3)]$ after dispersion on a carbon formvar grid (see the Supporting Information for preparation details). c,d) Representation of the negative mode ESI-MS spectra[17] of $Li_7[V_{15}O_{36}(CO_3)]$ in H_2O:CH_3CN (85:15): c) freshly prepared and dried $Li_7[V_{15}O_{36}(CO_3)]$; d) after treatment of $Li_7[V_{15}O_{36}(CO_3)]$ at 200 °C. The data show that both samples give the same main ion peaks and undergo fragmentation to the same extent.

therefore consisting of some tens of individual polyoxovanadate clusters. Mass spectroscopy of the $\{V_{15}O_{36}\}$ clusters before and after this high-temperature treatment confirms that the structure of the $\{V_{15}O_{36}\}$ clusters is retained after heating (i.e., they do not coalesce to form bulk oxide), which is also consistent with the results of FTIR (see Figure S3 and S4 in the Supporting Information).

Interestingly, $Li_7[V_{15}O_{36}(CO_3)]$ shows reversible redox behavior over the large voltage window 4.0–1.9 V versus Li/Li^+, when used in a half-cell with a metallic Li anode with 1 M $LiPF_6$ in ethylene carbonate (EC) + dimethyl carbonate (DMC) + ethyl methyl carbonate (EMC) (1:1:1, v/v) as the electrolyte. As illustrated by the cyclic voltammetry (**Figure 2**a), the polarization ΔE between the reduction and oxidization processes is small and the CVs of the first and second sweeps overlay well, indicating functional stability for the cathode and suggesting that $Li_7[V_{15}O_{36}(CO_3)]$ does not decompose during cycling. Meanwhile, the redox peaks are distributed in two voltage zones: 2.2–2.6 V and 3.3–3.7 V. In order to understand the cycling behavior of $Li_7[V_{15}O_{36}(CO_3)]$, galvanostatic charging–discharging was carried out to calculate the number of Li^+ ions translocating during these redox processes. As shown in the galvanostatic charging–discharging profiles in Figure 2b, $Li_7[V_{15}O_{36}(CO_3)]$ delivers an initial discharging capacity of 140 mA h g^{-1} at a current density of 50 mA g^{-1}. When charging back to 4.0 V versus Li^+/Li, a reversible charging–discharging capacity of 250 mA h g^{-1} is obtained for these $\{V_{15}O_{36}\}$ clusters. According to the equation:

$$Q = (nF)/(3.6M_w) = (96500n)/(3.6M_w) \quad (1)$$

where Q is the reversible charging–discharging capacity, n is the number of electrons passed during the redox reaction, and M_w is the molecular weight of $Li_7[V_{15}O_{36}(CO_3)]$ (M_w =1448.7 g mol^{-1}), the translocation of each Li^+ to/from the polyoxovanadate cluster contributes a capacity of around 18.5 mA h g^{-1}. As a result, we calculate that between seven and eight V^V centers (140/18.5) are electrochemically reduced to V^{IV} during the first discharging process, and that 13.5 V^V centers (250/18.5) undergo electrochemical oxidization during the subsequent charging process (and in the charge–discharge processes thereafter). The theoretical specific capacity for $Li_x[V_{15}O_{36}(CO_3)]$ within this voltage window can then be calculated by taking n to be 14 (the next nearest integer number of electrons), and feeding this number back into the equation above to find a theoretical specific capacity for $Li_x[V_{15}O_{36}(CO_3)]$ of 259 mA h g^{-1}.

$Li_7[V_{15}O_{36}(CO_3)]$ shows high rates performance when tested as a cathode over the voltage range 1.9–4.0 V (**Figure 3**a). The polarization of the discharging plateaus is not great when subjected to a high charging–discharging current density, and 170 mA h g^{-1} can be obtained at a high discharge rate of 2 A g^{-1}, and a specific capacity of around 140 mA h g^{-1} is possible at the even more extreme current density of 10 A g^{-1}. This excellent rates and cycling performance at high current density (with almost 100% Coulombic efficiency over 100 cycles, Figure 3c) could be due to the ultrafine size of the $Li_7[V_{15}O_{36}(CO_3)]$ active material (Figure 1b), and ensure a high power density output of 25.7 kW kg^{-1} with an energy density output of 370 W h kg^{-1} (Figure 3b). In terms of volumetric densities (and taking the crystal density of $Li_7[V_{15}O_{36}(CO_3)]$ to be 2.15 g cm^{-3}),

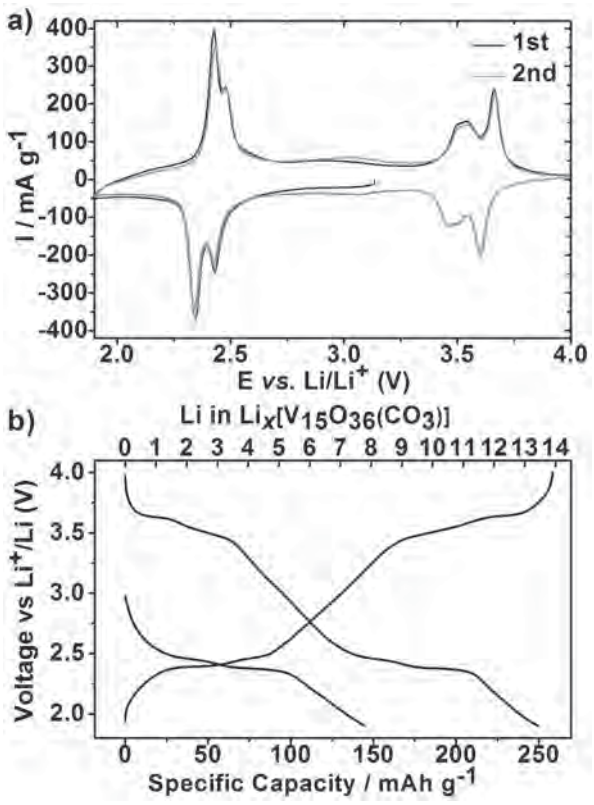

Figure 2. a) CV of the $Li_7[V_{15}O_{36}(CO_3)]$-based cathode at a scan rate of 0.2 mV s^{-1}, starting from open circuit voltage and scanning to low potential (1.9 V), before scanning back to high potential (4.0 V). b) The first discharge and second galvanostatic charge–discharge curves of $Li_7[V_{15}O_{36}(CO_3)]$ at a current density of 50 mA g^{-1} over the range 1.9–4.0 V.

$Li_7[V_{15}O_{36}(CO_3)]$ exhibits energy and power densities of 1.5 kW h L^{-1} and 55 kW L^{-1}.

The kinetics of the various reversible redox processes of $Li_7[V_{15}O_{36}(CO_3)]$ were studied by the potentiostatic intermittent titration techniques (PITT) method.[12,18] As shown in **Figure 4**, the chronoamperometric response of $Li_7[V_{15}O_{36}(CO_3)]$ indicated no obvious bell-shape variation, suggesting that Li-ion migration is not kinetically limited by a two-phase interface in these electrodes. In fact, all the current curves decay gradually during each potential step and almost follow a Cottrell-type law, indicative of a solid solution insertion process kinetically limited by Li^+ diffusion. This behavior is significantly different from the intercalation processes found in the bulk oxides commonly used in Li-ion batteries, such as the $LiMPO_4$[19] and $Li_xV_2O_5$ systems.[20] $Li_xV_2O_5$ generally displays four or five plateau regions, each one corresponding to a two-phase process, while $Li_7[V_{15}O_{36}(CO_3)]$ has similar redox behavior but corresponding to a solid solution insertion process. As a result, a methodology based on galvanostatic intermittent titration techniques (GITT) and electrochemical impedance spectroscopy (EIS) [21] can be used to estimate the apparent chemical diffusion coefficient of Li^+ in the $Li_7[V_{15}O_{36}(CO_3)]$-based cathode. As shown in Figure S6 (Supporting Information), the $D_{aap,Li}$ values are comparatively high over the voltage range 2.2–3.9 V, with values ranging from 1.4×10^{-10} to 2.3×10^{-7} cm^2 s^{-1}, showing that the mobility of Li^+ ions remains high in this material when compared to other bulk metal oxides such as $LiCoO_2$ (10^{-12} to 10^{-10} cm^2 s^{-1} over the voltage range 3.85–4.35 V)[22] and V_2O_5 (10^{-11} to 10^{-8} cm^2 s^{-1} over the voltage range 3.2–3.45 V).[23] The progressively decreasing concentration of vacant sites available for Li^+ as intercalation of Li^+ proceeds would cause a lower diffusion coefficient in $LiCoO_2$,[24] while the variation of diffusion coefficient with voltage in $Li_7[V_{15}O_{36}(CO_3)]$ suggests a decreasing number of uptake/removal sites for Li^+ on the surface of the cluster. $Li_7[V_{15}O_{36}(CO_3)]$ is an open-framework material consisting of multiple individual polyoxovanadate clusters, each of which has multiple vanadium centers undergoing redox cycling, and as such it may have a rather different Li-ion transportation mechanism to that displayed in traditional bulk metal oxide cathodes. The rapid diffusion of Li^+ in the $Li_7[V_{15}O_{36}(CO_3)]$-based cathodes suggests that the uptake/removal processes of Li ions in polyoxometalate-based batteries are somewhat easier than the intercalation/deintercalation processes at work in bulk metal oxides. Moreover, the electronic conductivity of the $Li_7[V_{15}O_{36}(CO_3)]$ cathode material was found to be 1.12×10^{-6} S cm^{-1} at 20 °C (Figure S7, Supporting Information), which also compares favorably with currently available cathode materials (around 1×10^{-9} S cm^{-1} for $LiFePO_4$ and around 1×10^{-6} S cm^{-1} for $LiCoO_2$).

Control experiments using equivalent loadings of $LiVO_3$ and V_2O_5 (two likely decomposition products of $Li_7[V_{15}O_{36}(CO_3)]$) showed that these simpler oxides of vanadium exhibit impaired and/or less stable behavior than $Li_7[V_{15}O_{36}(CO_3)]$ when used as the base materials for Li battery cathodes (see Figure S8 and S9 in the Supporting Information). Considering the reversibility of the charge–discharge processes of the $Li_7[V_{15}O_{36}(CO_3)]$-based electrodes, it thus seems likely that higher nuclearity polyoxometalate clusters are required in order to achieve the activity observed in the batteries studied herein. These control experiments also suggest that decomposition of the polyoxometalate clusters to these simpler oxides does not occur to a significant degree over the number of cycles studied. In a similar way, cathodes containing $Li_7[V_{15}O_{36}(CO_3)]$ that had been cycled in a battery ten times were extracted with water, and mass spectrometry was performed on the material dissolved out of these electrodes. These data (see Figure S10 in the Supporting Information) show that the molecular polyoxometalate cluster is still present in the cathode after multiple cycling events.

In conclusion, our studies of $Li_7[V_{15}O_{36}(CO_3)]$ have identified polyoxovanadates as a new class of potential cathode material for future high energy and power density Li-ion rechargeable batteries. Rapid lithium-ion diffusion and good electron conductivity in $Li_7[V_{15}O_{36}(CO_3)]$ should allow rapid charging and discharging of the resulting battery, and we have shown that a power density output of 25.7 kW kg^{-1} (55 kW L^{-1}) is possible with this material. In contrast to the bulk oxides traditionally used as cathode and anode materials in rechargeable batteries, the polyoxometalate investigated herein can undergo multi-electron reduction while still retaining its cluster structure. On account of the wealth of readily accessed polyoxometalate structures, we believe that this approach will provide great opportunity to optimize different functional materials to fulfill various electrochemical applications.

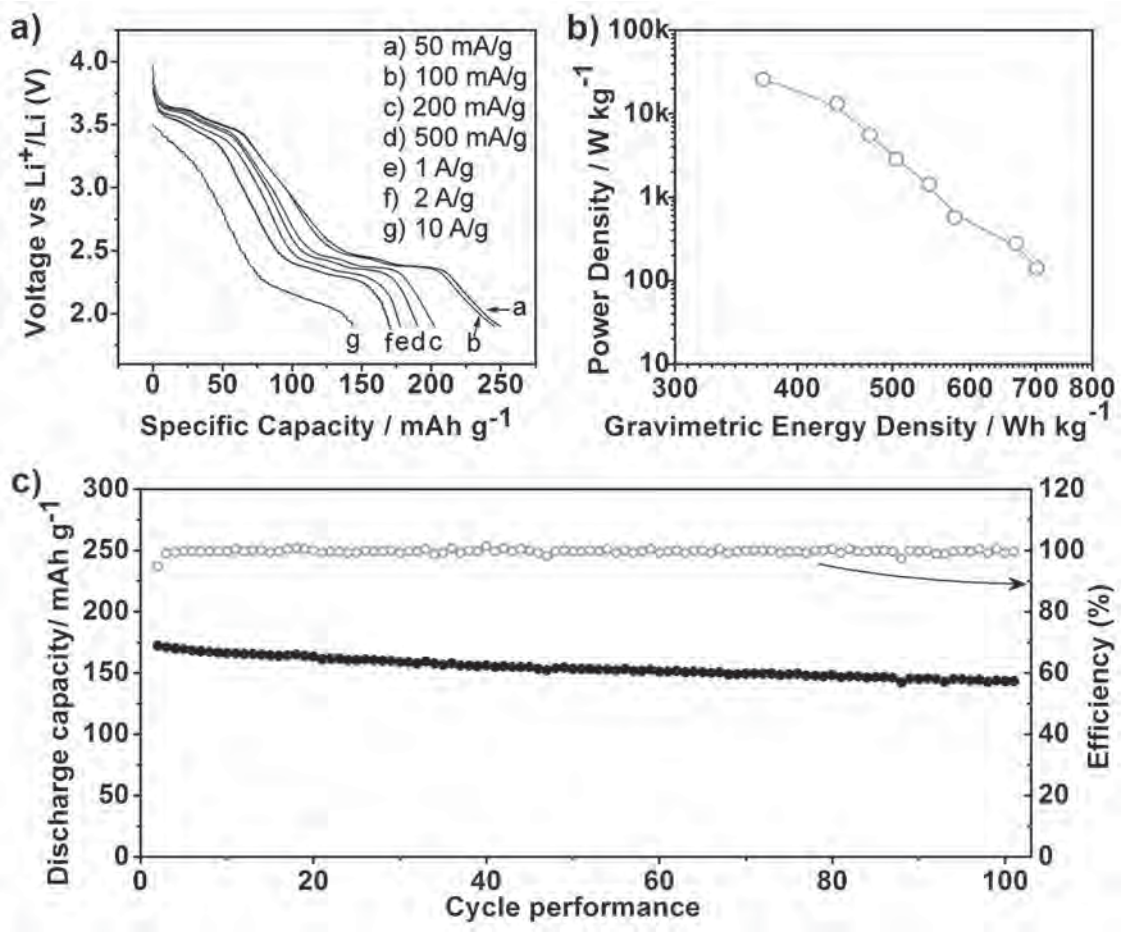

Figure 3. a) Discharge curves for $Li_7[V_{15}O_{36}(CO_3)]$ over the voltage range of 1.9–4.0 V versus Li^+/Li at different current densities. b) Ragone plot comparing the power and gravimetric energy densities based on the mass of $Li_7[V_{15}O_{36}(CO_3)]$. c) Cycle performance with Coulombic efficiency of $Li_7[V_{15}O_{36}(CO_3)]$ at the high current density of 2 A g^{-1} over 100 cycles.

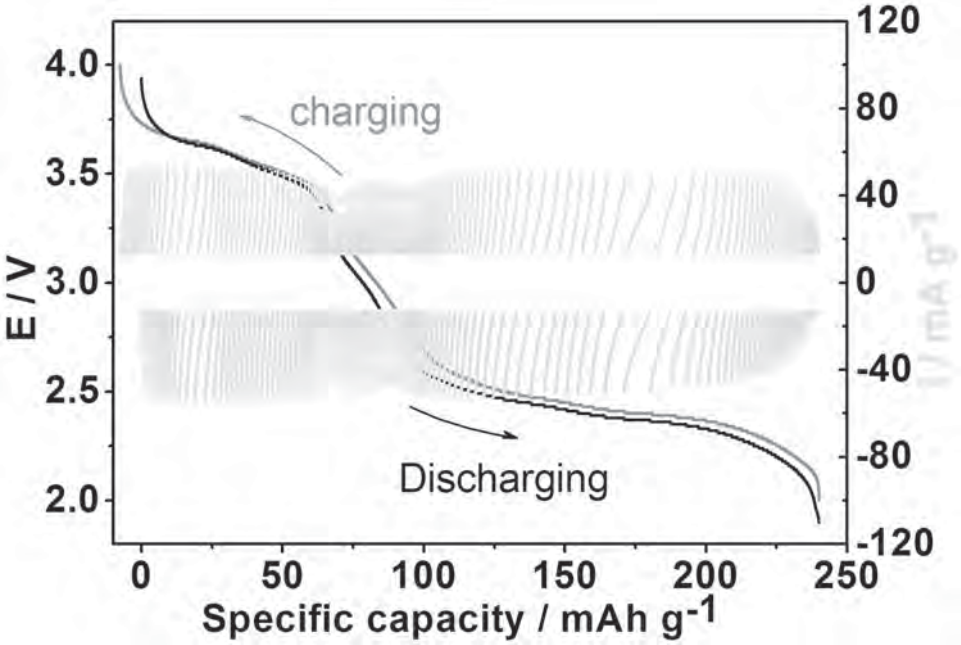

Figure 4. The chronoamperometric response of the $Li_7[V_{15}O_{36}(CO_3)]$-based electrode by the potentiostatic intermittent titration techniques method (PITT). An expansion of the zone between 50 and 120 mA h g^{-1} can be found in the Supporting Information (Figure S5).

Experimental Section

Synthesis of $Li_7[V_{15}O_{36}(CO_3)]$ and Characterization: $Li_7[V_{15}O_{36}(CO_3)]$ was prepared according to an adapted literature procedure.[17] TGA-DTA was carried out on a Pyris Diamond TG-DTA (PE Co., USA) to obtain the optimized treatment temperature in a constant flow of dry N_2 (50 mL min^{-1}) and a heating/cooling rate of 10 °C min^{-1}. Alumina crucibles were loaded with 5–10 mg of sample powder. The weight loss before 200 °C (see Figure S2 in the Supporting Information) is ascribed to the dehydration of $Li_7[V_{15}O_{36}(CO_3)]\cdot nH_2O$. The optimized treatment temperature was determined to be 200 °C and the samples were placed into a furnace to anneal at 200 °C for 10 h under N_2, and then were pulverized to a fine powder by ball milling after cooling to room temperature. The purity of the as-prepared and dehydrated samples was characterized by IR spectroscopy. The morphology of the dehydrated $Li_7[V_{15}O_{36}(CO_3)]$ powder was observed by field-emission scanning electron microscopy (SEM) (Hitachi S-4800) and transmission electron microscopy (TEM) (Hitachi JEM-2100, 200 kV). The structural stability of $Li_7[V_{15}O_{36}(CO_3)]$ was also investigated by mass spectroscopy which was collected using a Q-trap, time-of-flight MS (MicrOTOF-Q MS) instrument supplied by Bruker Daltonics Ltd. The detector was a time-of-flight, microchannel plate detector and all data were processed using the Bruker Daltonics Data Analysis 3.4 software, while simulated isotope patterns were investigated using Bruker Isotope Pattern software and Molecular Weight Calculator 6.45. The calibration solution used was Agilent ES tuning mix solution, Recorder No. G2421A, enabling calibration between approximately 100 *m*/*z* and 3000 *m*/*z*. This solution was diluted 60:1 with MeCN. Samples were introduced into the MS via direct injection at 180 µL h^{-1}. The ion polarity for all MS scans recorded was negative at 180 °C, with the voltage of the capillary tip set at 4000 V, collision cell RF 1250 Vpp, transfer time 90 µs, end plate offset at –500 V, funnel 1 RF at 300 Vpp and funnel 2 RF at 400 Vpp.

Electrochemical Testing: $Li_7[V_{15}O_{36}(CO_3)]$ crystals were placed into a furnace to anneal at 200 °C for 6 h under N_2, and then were pulverized to a fine powder by ball milling after cooling to room temperature. The cathodes were then prepared by mixing 70 wt% $Li_7[V_{15}O_{36}(CO_3)]$, 20 wt% acetylene black, and 10 wt% PVDF binder. The resulting slurries were coated onto Al foil current collectors by a doctor blade method and dried at 105 °C under vacuum overnight. Such a cathode, a lithium foil anode, a Cellgard2400 separator, and the electrolyte were then sealed into a CR2016-type coin cell. 1 M $LiPF_6$/ethylene carbonate (EC) + dimethyl carbonate (DMC) + ethyl methyl carbonate (EMC) (1:1:1, v/v) was used as the electrolyte. Cyclic voltammetry measurements were carried out over the voltage range 1.9–4.0 V at a scan rate of 0.2 mV s^{-1} using a multichannel potentiostat (VMP2, Bio-logic Instruments). The galvanostatic charge–discharge testing was conducted on a NEWARE BTS-5V/5 mA type battery charger (Shenzhen NEWARE Co., China) over the voltage range 1.9–4.0 V. All the cathodes used had mass loadings of around 1.2 mg cm^{-2}.

A detailed description of the conductivity testing, the cation insertion process, and the determination of the diffusion coefficient can be found in the Supporting Information.

Supporting Information

Supporting Information is available from the Wiley Online Library or from the author.

Acknowledgements

The authors gratefully acknowledge financial support from the EPSRC (Grant Nos. EP/H024107/1, EP/I033459/1, EP/J015156/1, EP/L023652/1), EVOBLISS EC 69722 and the University of Glasgow, National 973 Program (2015CB251102), the NSFC Key Project (U1305246, 21321062), and the NFFTBS (No. J1310024). The authors thank Dr. De-Liang Long (University of Glasgow) for useful discussions. M.D.S. thanks the University of Glasgow for a Kelvin–Smith Research Fellowship and L.C. thanks the Royal Society for a Wolfson merit award.

Received: March 5, 2015
Revised: May 24, 2015
Published online: July 14, 2015

[1] M. S. Whittingham, *Chem. Rev.* **2004**, *104*, 4271.
[2] a) J. W. Fergus, *J. Power Sources* **2010**, *195*, 939; b) B. Scrosati, J. Garche, *J. Power Sources* **2010**, *195*, 2419.
[3] V. Etacheri, R. Marom, R. Elazari, G. Salitra, D. Aurbach, *Energy Environ. Sci.* **2011**, *4*, 3243.
[4] a) H. Chen, C. P. Grey, *Adv. Mater.* **2008**, *20*, 2206; b) K. M. Shaju, P. G. Bruce, *Adv. Mater.* **2006**, *18*, 2330.
[5] a) S. Lee, Y. Cho, H.-K. Song, K. T. Lee, J. Cho, *Angew. Chem. Int. Ed.* **2012**, *51*, 8748; b) D. K. Kim, P. Muralidharan, H.-W. Lee, R. Ruffo, Y. Yang, C. K. Chan, H. Peng, R. A. Huggins, Y. Cui, *Nano Lett.* **2008**, *8*, 3948.
[6] a) C. Delmas, M. Maccario, L. Croguennec, F. Le Cras, F. Weill, *Nat. Mater.* **2008**, *7*, 665; b) A. K. Padhi, K. S. Nanjundaswamy, J. B. Goodenough, *J. Electrochem. Soc.* **1997**, *144*, 1188; c) J. M. Clark, S.-i. Nishimura, A. Yamada, M. S. Islam, *Angew. Chem. Int. Ed.* **2012**, *51*, 13149.
[7] a) B. Kang, G. Ceder, *Nature* **2009**, *458*, 190; b) Y. Wang, G. Cao, *Adv. Mater.* **2008**, *20*, 2251.
[8] B. Lung-Hao Hu, F.-Y. Wu, C.-T. Lin, A. N. Khlobystov, L.-J. Li, *Nat. Commun.* **2013**, *4*, 1687.
[9] a) X. P. Gao, H. X. Yang, *Energy Environ. Sci.* **2010**, *3*, 174; b) M. S. Islam, C. A. J. Fisher, *Chem. Soc. Rev.* **2014**, *43*, 185.
[10] a) N. Kawasaki, H. Wang, R. Nakanishi, S. Hamanaka, R. Kitaura, H. Shinohara, T. Yokoyama, H. Yoshikawa, K. Awaga, *Angew. Chem. Int. Ed.* **2011**, *50*, 3471; b) H. Yoshikawa, C. Kazama, K. Awaga, M. Satoh, J. Wada, *Chem. Commun.* **2007**, 3169; c) H. Yoshikawa, S. Hamanaka, Y. Miyoshi, Y. Kondo, S. Shigematsu, N. Akutagawa, M. Sato, T. Yokoyama, K. Awaga, *Inorg. Chem.* **2009**, *48*, 9057; d) Y.-G. Chen, C.-G. Wang, X.-Y. Zhang, D.-M. Xie, R.-S. Wang, *Synth. Met.* **2003**, *135–136*, 225; e) Y. Ji, J. Hu, L. Huang, W. Chen, C. Streb, Y.-F. Song, *Chem. Eur. J.* **2015**, *21*, 6469; f) S. Herrmann, C. Ritchie, C. Streb*Dalton Trans.* **2015**, *44*, 7092; g) Y. Ji, L. Huang, J. Hu, C. Streb, Y.-F. Song, *Energy Environ. Sci.* **2015**, *8*, 776.
[11] a) Z. Zhang, H. Yoshikawa, K. Awaga, *J. Am. Chem. Soc.* **2014**, *136*, 16112; b) Y. Lin, Q. Zhang, C. Zhao, H. Li, C. Kong, C. Shen, L. Chen, *Chem. Commun.* **2015**, *51*, 697; c) J. Qian, M. Zhou, Y. Cao, X. Ai, H. Yang, *Adv. Energy Mater.* **2012**, *2*, 410.
[12] G. Férey, F. Millange, M. Morcrette, C. Serre, M.-L. Doublet, J.-M. Grenèche, J.-M. Tarascon, *Angew. Chem. Int. Ed.* **2007**, *46*, 3259.
[13] a) H. N. Miras, J. Yan, D.-L. Long, L. Cronin, *Chem. Soc. Rev.* **2012**, *41*, 7403; b) H.-Y. Zang, J.-J. Chen, D.-L. Long, L. Cronin, H. N. Miras, *Adv. Mater.* **2013**, *25*, 6245.
[14] C. Busche, L. Vila-Nadal, J. Yan, H. N. Miras, D.-L. Long, V. P. Georgiev, A. Asenov, R. H. Pedersen, N. Gadegaard, M. M. Mirza, D. J. Paul, J. M. Poblet, L. Cronin, *Nature* **2014**, *515*, 545.
[15] a) B. Rausch, M. D. Symes, G. Chisholm, L. Cronin, *Science* **2014**, *345*, 1326; b) M. D. Symes, L. Cronin, *Nat. Chem.* **2013**, *5*, 403.
[16] a) H. Wang, S. Hamanaka, Y. Nishimoto, S. Irle, T. Yokoyama, H. Yoshikawa, K. Awaga, *J. Am. Chem. Soc.* **2012**, *134*, 4918; b) Y. Nishimoto, D. Yokogawa, H. Yoshikawa, K. Awaga, S. Irle, *J. Am. Chem. Soc.* **2014**, *136*, 9042; c) H. Wang, T. Yamada, S. Hamanaka, H. Yoshikawa, K. Awaga, *Chem. Lett.* **2014**, *43*,

1067; d) H. Yang, T. Song, L. Liu, A. Devadoss, F. Xia, H. Han, H. Park, W. Sigmund, K. Kwon, U. Paik, *J. Phys. Chem. C* **2013**, *117*, 17376.
[17] a) H. N. Miras, E. F. Wilson, L. Cronin, *Chem. Commun.* **2009**, *1297*; b) E. F. Wilson, H. N. Miras, M. H. Rosnes, L. Cronin, *Angew. Chem. Int. Ed.* **2011**, *50*, 3720; c) A. Müller, M. Penk, R. Rohlfing, E. Krickemeyer, J. Döring, *Angew. Chem. Int. Ed. Engl.* **1990**, *29*, 926.
[18] N. Recham, J. N. Chotard, L. Dupont, C. Delacourt, W. Walker, M. Armand, J.-M. Tarascon, *Nat. Mater.* **2010**, *9*, 68.
[19] C. A. J. Fisher, V. M. Hart Prieto, M. S. Islam, *Chem. Mater.* **2008**, *20*, 5907.
[20] X. Rocquefelte, F. Boucher, P. Gressier, G. Ouvrard, *Chem. Mater.* **2003**, *15*, 1812.
[21] W. Weppner, R. A. Huggins, *Annu. Rev. Mater. Sci.* **1978**, *8*, 269.
[22] M. D. Levi, G. Salitra, B. Markovsky, H. Teller, D. Aurbach, U. Heider, L. Heider, *J. Electrochem. Soc.* **1999**, *146*, 1279.
[23] S.-I. Pyun, J.-S. Bae, *Electrochim. Acta* **1996**, *41*, 919.
[24] A. Van der Ven, J. Bhattacharya, A. A. Belak, *Acc. Chem. Res.* **2012**, *46*, 1216.